



COPY RIGHT



ELSEVIER
SSRN

2021 IJEMR. Personal use of this material is permitted. Permission from IJEMR must be obtained for all other uses, in any current or future media, including reprinting/republishing this material for advertising or promotional purposes, creating new collective works, for resale or redistribution to servers or lists, or reuse of any copyrighted component of this work in other works. No Reprint should be done to this paper, all copy right is authenticated to Paper Authors

IJEMR Transactions, online available on 29th Mar 2021. Link

[:http://www.ijiemr.org/downloads.php?vol=Volume-10&issue=ISSUE-03](http://www.ijiemr.org/downloads.php?vol=Volume-10&issue=ISSUE-03)

DOI: 10.48047/IJEMR/V10/I03/127

Title Application of Enhanced Sine Cosine Algorithm for Optimal Allocation of PV- DG and DSTATCOM in Distribution Systems

Volume 10, Issue 03, Pages: 594-615

Paper Authors

Montaser Abd El Sattar, Amal M. Abd El Hamed, Adel A. Elbaset , Mohamed Ebeed



USE THIS BARCODE TO ACCESS YOUR ONLINE PAPER

To Secure Your Paper As Per **UGC Guidelines** We Are Providing A Electronic Bar Code

Application of Enhanced Sine Cosine Algorithm for Optimal Allocation of PV- DG and DSTATCOM in Distribution Systems

Montaser Abd El Sattar^{1,*}, Amal M. Abd El Hamed², Adel A. Elbaset³, Mohamed Ebeed⁴

¹Department of Electrical Engineering, Faculty of Engineering, South Valley University, Qena 83523, Egypt.

²Electricity Department, Faculty of Technology and Education, Sohag University, Sohag, Egypt

³Electrical Engineering Department, Faculty of Engineering, Minia University, El-Minia, Egypt

⁴Department of Electrical Engineering, Faculty of Engineering, Sohag University, Sohag, Egypt

*Corresponding: Montaser Abd El Sattar (Montaser.A.Elsattar@eng.svu.edu.eg)

Abstract

The allocation and optimization of renewable energy and shunt compensators remains a challenging task to enhance the performance of system efficiently. This paper suggests a new methodology to determine the optimal placement and ratings of the Photovoltaic based distributed generator (PV- DG) and Distribution Static compensator (DSTATCOM) in radial distribution systems. An Enhanced Sine cosine algorithm (ESCA) is applied to solve the allocation problem of the PV- DG and DSTATCOM. The ESCA is proposed for improvement the searching capabilities of the conventional Sine Cosine Algorithm (SCA) by using the Levy Flight Distribution (LFD) and adaptive operator. to demonstrates effectiveness of the proposed algorithm, it has been tested on IEEE 33 and IEEE 69 bus systems for loss minimization by PV-DG and the obtained results are compared with other algorithm. The ESCA is applied for optimal inclusion assigning the PV- DG and DSTATCOM for a multi-objective function which comprises of three objective functions including the power loss reduction, voltage profile improvement and voltage stability enhancement. The outcomes reveal to that optimal inclusion of the PV- DG and DSTATCOM can enhance the performance of the system considerably. In addition of that the proposed algorithm is superior for solving the allocation problem compared with the state-of-the-arts algorithms.

Keywords: PV, Distribution System, Power Losses, Renewable Energy, Voltage Profiles.

1. Introduction

The radial distribution system (RDS) comprise various loads, thus, RDS has pauper power quality in terms of system power losses, voltage coil, and system stability [1]. Reactive power restitution is required to get better power quality in RDS. Improving power quality in

some cases, hence power resources need to be included in RDS to achieve rise power quality [2].

At present, the bulk of power generation is produced by generators based on fossil fuels such as gas, and small turbines [3]. Renewable energy based DG [4] Such as wind turbines

(WT), photovoltaic (PV) and small hydroelectric generators besides energy efficiency. [5] It has been recognized worldwide as an effective pathway to avoid the problems associated with traditional energy sources. Besides, the concept of small grid is also seen as a promising solution for optimum utilization of energy resources [6] and to enhance the flexibility of power distribution systems [7].

Photovoltaic energy based on photovoltaic is a new renewable energy resource that has been widely integrated into distribution networks to achieve many benefits to enhance the environmental, technical and economic benefits [8] [9]. The PV modules convert the solar radiation into DC energy by its solar cells and then an inverter is used to invert the DC voltage into AC voltage. There are two options for connecting the PV system, the first installation is to connect the photovoltaic power to the electrical grid which is known as the PV system to the grid, and the other connection is regulated by feeding an independent system known as the off-grid PV system. Several improvements have been used to set the optimum capacity for PV modules such as; Genetic algorithm [10, 11], artificial bee colony [12], grasshopper optimization algorithm [13], moth flame optimizer [14], lightning attachment procedure optimization [15], backtracking search optimization [16] and ant lion optimization [17].

SCA technology is a new improvement technology he introduced [18]. The prime deficiency of the SCA is her stagnant and native idealism. An amended version of SCA

has been proposed to enhance the exploration and exploitation of traditional SCA. The ISCA relies on Levy's flight distribution and adaptive operators to enhance the search abilities of the primary SCA.

This paper proposes a new methodology to solve the renewable energy planning optimization problem based on the Enhanced sine Cosine algorithm (ESCA), in addition, the paper effects of combine DSTATCOM and PV modules into the distribution network. The proposed algorithm was tested on 33 and 69 vector radial distribution systems. The studied objective function includes minimizing power losses, minimizing voltage deviations and improving voltage stability. The results obtained via the proposed algorithm were compared with other results to highlight its benefits in reducing the total energy loss.

2. Problem Formulation

In the case of inclusion of the hybrid PV-DG and DSTATCOM as depicted. Eq. (1-3) is used to obtain the power flow solution in the RDS with inclusion PV units and DSTATCOM shown in Fig. 1.

$$P_{n+1} = P_n - P_{L,n+1} - R_{n,n+1} \left(\frac{P_n^2 + jQ_n^2}{|V_n|^2} \right) + P_{PV}$$

$$Q_{n+1} = Q_n - Q_{L,n+1} - X_{n,n+1} \left(\frac{P_n^2 + jQ_n^2}{|V_n|^2} \right) + Q_{DSTAT}$$

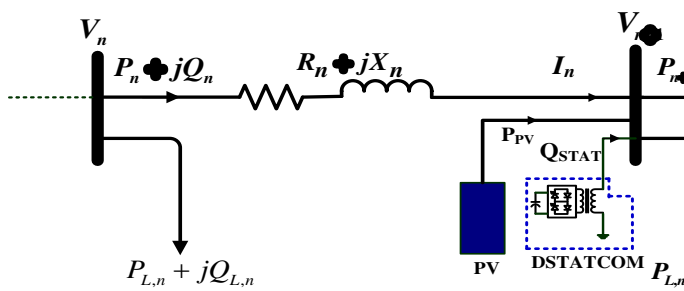


Fig.1 Schematic graph of system with PV and DSTATCOM

where, $X_{n,n+1}$ and $R_{n,n+1}$ are reactance and resistance of the line between buses n and $n + 1$, respectively. Q_n and P_n are the real and reactive powers flows, respectively. The active and reactive power losses are given as follows:

$$P_{loss(n,n+1)} = R_{n,n+1} \left(\frac{P_n^2 + jQ_n^2}{|V_n|^2} \right) \quad (3)$$

The voltage stability index can be found as follows.

$$VSI_{(n+1)} = |V_n|^4 - 4(P_{mn+1}X_n - Q_{n+1}R_n)^2 - 4(P_{mn+1}X_n + Q_{n+1}R_n)|V_n|^2 \quad (4)$$

where, $VSI_{(n+1)}$ is the voltage stability index, voltage deviations of RDS can be found as follows:

$$VD = \sum_{g=1}^n |V_n - 1| \quad (5)$$

where, n is number of system nodules.

3. Objective Function

In this paper, the purpose of inclusive PV and DSTATCOM is to reduce power losses,

improve system stability, and improve the voltage profile. So, the objective function is subedit as follows:

$$\Phi = \lambda_1 \Phi_1 + \lambda_2 \Phi_2 + \lambda_3 \Phi_3 \quad (6)$$

where, λ_1 , λ_2 and λ_3 are weighting factors. collection of the weight factors assigned to all effects must add up to one as:

$$|\lambda_1| + |\lambda_2| + |\lambda_3| = 1 \quad (7)$$

Φ_1 is the first objective of the multi objective assignment which total active power losses decrease and it can be found as follows:

$$\Phi_1 = \frac{P_{T,loss}}{(P_{T,loss})_{base}} \quad (8)$$

where, $P_{T,loss}$ are the total active power losses in system. The base bed icon ticks the basic state of the network (without PV and DSTATCOMs). Φ_2 exemplify the improvement the voltage profile, which is persuaded by decrease the sum of the voltage deviations in RDS and can be given as follows:

$$\Phi_2 = \frac{VD}{(VD)_{base}} \quad (9)$$

where, Φ_3 The improvement of the voltage stability that can be achieved by improving the voltage stability index (VSI) is represented as follows:

$$\Phi_3 = \frac{1}{\sum_{i=1}^{nb} |VSI(i)|_{base}}$$

4. System Constraints

The system constraints are classified as follows:

4.1 Equality Constraints

Equality constraints contain flows of active and reactive forces which can be given as follows:

$$P_s + \sum_{i=1}^{np} P_{PV} = \sum_{h=1}^n P_D (h) + \sum_{j=1}^{nl} P_{loss} (j) \quad (11)$$

$$Q_s + \sum_{i=1}^{nc} Q_{DSTATCOM} (i) = \sum_{h=1}^n Q_D (h) + \sum_{j=1}^{nl} Q_{loss} (j) \quad (12)$$

where, P_s and Q_s It is the active and reactive powers supply at the substation, respectively. P_D and Q_D are Active and reactive load, respectively. nl is the number of transmission lines in RDS. nc is the number of DSTATCOM. np is the number of PV modules.

4.2 Inequality Constraints

$$V_{min} \leq V_i \leq V_{max} \quad (1, 3)$$

$$\sum_{i=1}^{nc} Q_{DSTATCOM} (i) \leq \sum_{i=1}^n Q_D (i) \quad (1, 4)$$

$$\sum_{i=1}^{np} P_{PV} (i) \leq \sum_{i=1}^n P_D (i) \quad (1, 5)$$

$$I_n \leq I_{max,n} \quad n = 1, 2, 3, \dots, nb \quad (16)$$

where, V_{min} and V_{max} are the lower and upper voltage limits. P_D and Q_D are the active and reactive loads. $Q_{DSTATCOM}$ Reactive force is injected by DSTATCOM. P_{PV} is injected reactive power by PV modules.

5. Optimization Algorithm

SCA It is optimization algorithm. SCA is a population based algorithm and its combinations about the best solutions are updated based on a random process using cosine functions as shown in Fig.2 which can be described as follows [18, 19]:

$$X_i^{t+1} = \begin{cases} X_i^t + y_1 \times \sin(y_2) \times |y_3 X_{best}^t - X_i^t| \\ X_i^t + y_1 \times \cos(y_2) \times |y_3 X_{best}^t - X_i^t| \end{cases} \quad (1, 7)$$

where, t is the iteration X_i^{t+1} and X_i^t is the population positions at t th and $(t+1)$ th iteration at the i th dimension, respectively. X_{best}^t represents the best position. y_2, y_3 and y_4 are random numbers during range $[0, 1]$. y_1 exemplify an adaptive parameter that is instituted as follows:

$$y_1 = k - t \times \frac{K}{t_{max}} \quad (18)$$

where, k is a fixed value. T_{max} is The maximum number of iterations. We must dot out that Eq. (18) characterize the main

where, K_{max} and K_{min} are the upper and lower sect width limits. t is the current iteration and T_{max} is the maximum number of iterations.

6. Simulation Results

In order to determine the proposed SCA features and the enhanced SCA algorithm and examine their performance, two radial distribution systems were selected IEEE 33 and IEEE 69-bus system. The load model for distribution systems is assumed to be a static power load [20]. The line diagram of a system

considered is shown in Fig. 4 and Fig. 5. The proposed algorithm is a code using MATLAB 2019b and simulations are present on a Dell computer of an intel core TM I7 processor with a frequency of 3.20 GHz and 32.0 GB of RAM. Back/forward sweep algorithm [21]- [22], its affinity is strong and assured [20], Solve calculations of energy flow. Specifications parameters and primary power flow results without any RESs are shown in Table 1 and Table 2.

Table 1. System specification and initial power flow.

Item	Value	Value
System Specifications:		
NB	33	69
Npr	32	68
Vsys (kV)	12.66	12.66
Base MVA	100	100
S_{Load} (MVA)	$3.715 + j2.300$	$3.802 + j2.694$
$P_{Total_{loss}}$ (kW)	210.84	225
$Q_{Total_{loss}}$ (kVar)	143.022	102.198
V_{min} (p.u) @ bus	0.90378, 18	0.90919, 65

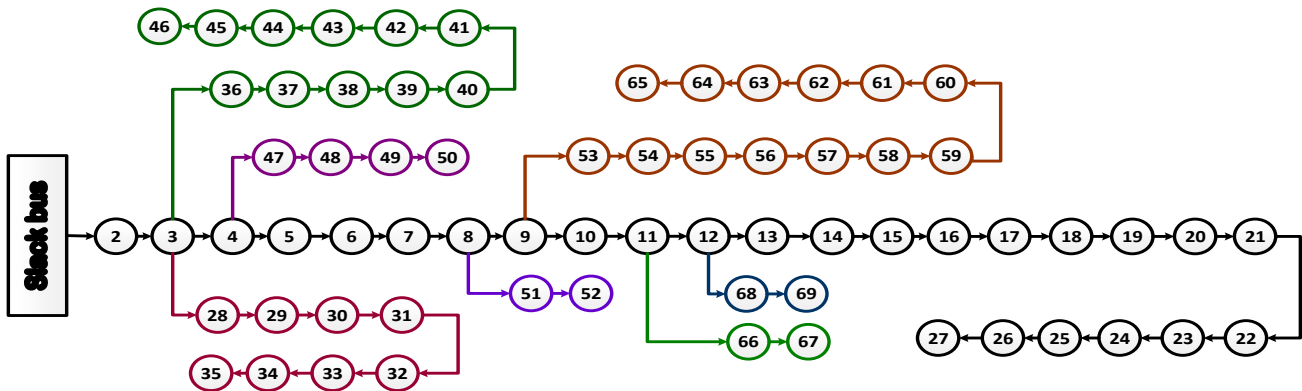


Fig 4. Single line diagram of IEEE 69 bus system

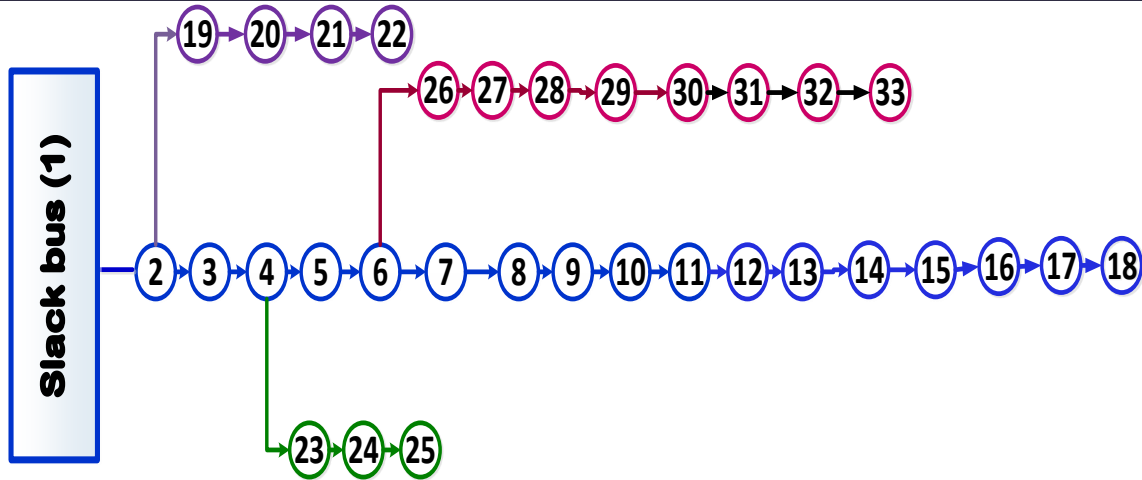


Fig 5. Single line diagram of IEEE 33 bus system

Table 2. Input parameters used in numerical simulations.

Item	Set value(s)
SCA-ESCA parameters:	
Niter,max	100
Npop	50
Nruns	50
System inequality constraints:	
Bus voltage limits (p.u.)	$\pm 5\%*$
PV size limits (MVA)	$0 \leq SPV \leq 3$
PV Power Factor limits [24]	$1 \leq PFPV \leq 1$

7. The First Case Study 33 Bus System.

The first case system over the proposed ESCA is the 33-bus system. Its total load is 3720 kW and 2300 kVA at voltage level of 12.66 kV. Table 3,4 describes the effects of fixation of different types and numbers of PV on system performance. The superiority of the ESCA has been demonstrated in selecting the optimal sites and size of the photovoltaic compared to those obtained. are shown in Table 5,6,7. Significant reduction in active energy loss was enhanced for both PV. In addition, a marked improvement in the voltage profile and system stability was achieved, as shown in

Fig.6 and Fig.7, respectively. In the first method, bus number 6 has been suggested as the optimal location for PV. The optimum size for PV is 2590.2 kW. The energy power loss resulting from the proposed technology has decreased to 111.02 kW.

In the second method, the integration of multiple PV-DGs (**two and three modules**) is considered, and their effects are investigated. In the case of two PV-DGs, buses 13 and 30 were selected as ideal sites for PV-DGs integration with capacities of 851.4817 kW and 1154 kW respectively. On the other hand, the optimal locations for three PV-DGs are buses 30, 13 and 24 and the PV capacities are 1053.5, 802

and 1091.3 kW respectively. It is noteworthy that the active power loss was significantly

reduced to 87.165 kW and 72.785 kW by two PV-DGs and three PV-DGs, respectively.

Table 3. The results of installing of PV units in the first system.

Items	Without -PV	With PV					
		One PV		Two PV		Three PV	
		ESCA	SCA	ESCA	SCA	ESCA	SCA
Total losses (kW)	210.98	111.02	111.016	87.165	87.343	72.785	78.928
Minimum voltage	0.90378 @ bus 18	0.94237 @ bus 18	0.94231 @ bus 18	0.96839 @ bus 33	0.96626 @ bus 33	0.96867 @ bus 33	0.97711 @ bus 33
Maximum voltage	0.99703 @ bus 2	0.99858 @ bus 2	0.99858 @ bus 2	0.99826 @ bus 2	0.99822 @ bus 2	0.99882 @ bus 2	0.99910 @ bus 2
PV size in kW (Location)	-	2590.2 (6)	2585.7 (6)	851.4817(13), 1154 (30)	832.4591(13), 1096 (30)	1053.5 (30), 802 (13), 1091.3 (24)	1100.8 (24), 1195 (12), 1151.0 (30)
VSI	25.5401	28.5219	28.5166	29.3803	29.2442	29.6167	30.4819
VD (p.u)	1.8044	0.9237	0.9252	0.6786	0.7156	0.6167	0.3865

Table 4. Results of optimized allocation of PV units in 33 bus

Items	Without -PV			With Multi-Objective Function			
	ESCA			SCA			
	PV1	PV2	PV3	PV1	PV2	PV3	
Total losses (kW)	210.98	111.012	87.252	72.885	111.016	87.560	76.664
Minimum voltage	0.90378 @ bus 18	0.94237 @ bus 18	0.96425 @ bus 18	0.96772 @ bus 33	0.94231 @ bus 18	0.96533 @ bus 18	0.95496 @ bus 18

Maximum voltage	0.99703 @ bus 2	0.99858 @ bus 2	0.99830 @ bus 2	0.99882 @ bus 2	0.99858 @ bus 2	0.99835 @ bus 2	0.99857 @ bus 2
PV size in kW (Location)	-	2590.2 (6)	1104.4(30), 957 (12)	11091 (24), 838 (13), 1006.2(30)	2585.7 (6)	947.3237 (12), 1215 (30)	795.8191(11), 831 (31), 896.2417 (24)
VSI (p.u)	25.5401	28.5219	29.7753	29.6395	28.5166	29.6288	29.0059
VD (p.u)	1.8044	0.9237	0.5720	0.6106	0.9252	0.6126	0.7840

Table 5. A comparative results for incorporating **Single PV** in 33-bus system

Technique	Without	GA [23]	PSOPC[24]	EVPSO[24]	AEPSO [24]	ADPSO [24]	DAPSO [24]	Analytical [25]	GA [26]
P_{loss} (KW)	210.98	105.481	136.75	140.19	131.43	129.53	127.17	111.24	132.64
Location	-	6	15	11	14	13	8	6	6
Size (kVA)	-	2580	763	1000	1200	1210	1212	2490	2380

Technique	BSOA [16]	ESCA
P_{loss} (KW)	118.12	111.02
Location	8	6
Size (kVA)	1857.5	2590.2

Table 6. A comparative results for incorporating **Two PV** in 33-bus system

Technique	Without	[28]MINLP	Exhaustive OPF [29]	EA-OPF[29]	EA[29]	Hybrid[30]	PSO[30]	[31]IA	ESCA
P_{loss} (KW)	210.98	87.167	87.17	87.17	87.172	87.280	87.170	87.550	87.165
Location	-	13	13	13	13	13	13	12	13
Size (kVA)	-	30	30	30	30	30	30	30	30
	-	850, 1150	852, 1158	852, 1158	844, 1149	830, 1110	850, 1160	1020, 1020,	851.4817, 1154

Table 7. A comparative results for incorporating **Three PV** in 33-bus system

Technique	Without	[28]MINLP	Exhaustive OPF [29]	EA-OPF[29]	EA[29]	Hybrid[30]	PSO[30]	IA[31]	ESCA
P_{loss} (KW)	210.98	105.481	136.75	140.19	131.43	129.53	127.17	111.24	132.64
Location	-	13	13	13	13	13	13	13	30

		24	24	24	24	24	24	24	13
		30	30	30	30	30	30	30	24
Size	-	800,	802,	802,	798,	790,	770,	900,	1053.5
(kVA)		1090,	1091,	1091,	1099,	1070,	1090,	900,	,
		1050	1054,	1054	1050	1010	1070	900	802,
									1091.3

8. The Second Case Study 69 Bus System.

In this case, optimization results are obtained with ESCA mono and multi-modulated PV summarized in Table 8. The voltages and VSI voltages profiles are also illustrated in Fig.8 and Fig.9, respectively. The branch active energy loss profile is shown in Table 9. In the first method, a renewable energy integration is considered as (PV), bus 61 was nominated as the best location for the installation of the 1,872.7 kW PV array. The optimized layout of the PV module greatly reduces the active power loss, improves the voltage profile and the system stability so that the minimum bus voltage is 0.96829 p.u and VSI is 64.621 p.u.

In the second method, the optimal planning of renewable energy is examined taking into account the integration of multiple renewable energy. In the case of the two PV DGs, bus number 18 and 61 were nominated as the best locations, and the optimum capacity of the PV DGs is 531.26 kW and 1781 kW, respectively. It is noted that the

input of two PV DGs successfully participates in reducing the active power losses to 71.675 kW, and increasing the minimum voltage point to 0.97893 p.u. And VSI to 66.021p.u. Where the active power loss is reduced to 69.449 kW with three PV DGs power stations. Moreover, the system bus voltage profile was significantly improved by a precise uniform pattern as in Fig.8, which was confirmed by improvement in the minimum value of bus voltages before and after connection. The best value of power losses (for a moment, 83,224 kW with one PV) obtained by the proposed algorithm is lower than the best values shown in previous works. This reveals the efficiency of the algorithm developed over other methods to solve the problem of optimal allocation of renewable energy in distribution networks. Table 10,11,12. Comparative results of incorporating PV into a 69 bus system. Figures. 10, 11, 12, Figures 13, 14, 15. From the affinity graph, it can be seen that the objective value (total energy loss) converges rapidly in ESCA.

Table 8. The results of installing of PV units in the second system.

Items	Without - PV	With PV					
		One PV		Two PV		Three PV	
		ESCA	SCA	ESCA	SCA	ESCA	SCA

Total losses (kW)	225	83.222	83.231	71.675	72.201	69.484	70.757
Minimum voltage	0.90919 @ bus 65	0.96829 @ bus 27	0.96819 @ bus 27	0.97893 @ bus 65	0.98169 @ bus 65	0.97938 @ bus 65	0.97478 @ bus 65
Maximum voltage	0.99997 @ bus 2	0.99997 @ bus 2	0.99997 @ bus 2	0.99997 @ bus 2	0.99998 @ bus 2	0.99998 @ bus 2	0.99998 @ bus 2
PV size in kW (Location)	-	1872.7 (61)	1856.7 (61)	531.2598 (18), 1781 (61)	1856.1 (61), 566 (16)	596.0304 (11), 381 (18), 1719.0 (61)	1601.9 (61), 420 (19), 465.0150 (9)
VSI (p.u)	61.2181	64.6212	64.5925	66.0295	66.3084	66.3258	65.8222
VD (p.u)	1.8374	0.8729	0.8805	0.5002	0.4280	0.4241	0.5549

Table 9. Results of optimal allocation of PV-DGs.

Items	Without -PV		With Multi-Objective Function					
			ESCA			SCA		
			PV1	PV2	PV3	PV1	PV2	PV3
Total losses (kW)	225	89.230	77.605	74.412	89.393	79.677	77.635	
Minimum voltage	0.90919 @ bus 65	0.97072 @ bus 27	0.99087 @ bus 65	0.98810 @ bus 65	0.97075 @ bus 27	0.99211 @ bus 65	0.99179 @ bus 65	
Maximum voltage	0.99997 @ bus 2	0.99997 @ bus 2	1.00118 @ bus 17	0.99998 @ bus 2	0.99997 @ bus 2	1.00298 @ bus 15	0.99998 @ bus 2	
PV size in kW (Location)	-	2293.4 (61)	743.7399 (18), 2096 (61)	576.8192 (54), 1900 (61), 601.1664 (22)	2299.1 (61)	827.4227 (16), 2119 (61)	2128.2 (61), 716 (16), 705.0186 (3)	
VSI (p.u)	61.2181	65.3700	67.2296	67.1408	65.3645	66.9367	67.1311	

VD (p.u)	1.8374	0.6766	0.2002	0.2150	0.6780	0.2672	0.2170
-----------------	--------	--------	--------	--------	--------	--------	--------

Table 10. A comparative results for incorporating **Single PV** in 69-bus system

Technique	Without	MINLP[28]	Exhaustive [29]OPF	EA-OPF[29]	[33]HACO	Hybrid[30]	PSO[30]	GA [10]	GA [26]
P _{loss} (KW)	225	83.222	83.23	83.23	83.323	83.222	83.372	83.222	132.6
Location	-	61	61	61	61	61	61	61	61
Size (kVA)	-	1870	1870	1870	1872	1810	1870	1794	1819.6
Technique	ESCA								
P _{loss} (KW)	83.222								
Location	61								
Size (kVA)	1872.7								

Table 11. A comparative results for incorporating **Two PV** in 69-bus system

Technique	Without	MINLP[28]	GA [26]	CSA [34]	SGA [34]	PSO [34]	MTLBO [32]	GA [10]	ESCA
P _{loss} (KW)	225	71.693	71.7912	76.4	82.9	78.8	71.776	84.233	71.675
Location	-	17	61	22	17	14	17	1	18
Size (kVA)	-	61	11	61	61	62	61	62	61
Size (kVA)	-	510, 1780	1777, 555	600, 2100	1000, 2400	700, 2100	519.705, 1732.004	6, 1794	531, 2598, 1781

Table 12. A comparative results for incorporating **Three PV** in 69-bus system

Technique	Without	EA[29]	MTLBO[32]	KHA [35]	Hybrid[30]	PSO [34]	ESCA
P _{loss} (KW)	225	69.62	69.539	69.56	69.52	69.541	69.484
Location	-	11	11	12	11	11	11
Size (kVA)	-	18	18	22	17	17	18
Size (kVA)	-	61	61	61	62	61	61
Size (kVA)	-	467, 380, 1795	493, 378, 1672	496, 311, 1735	510, 380, 1670	460, 440, 1700	596.0304, 381, 1719.0

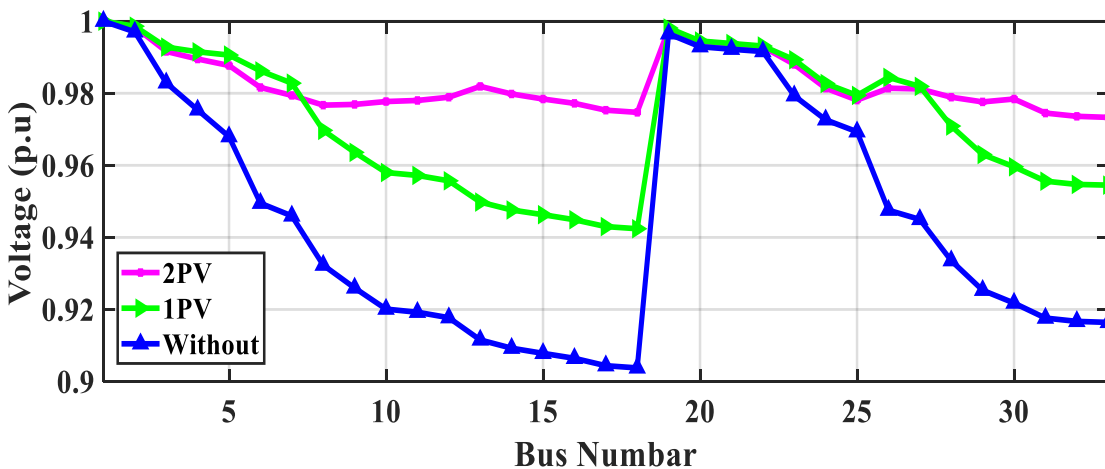


Fig .6. Voltage profile of the 33 bus system.

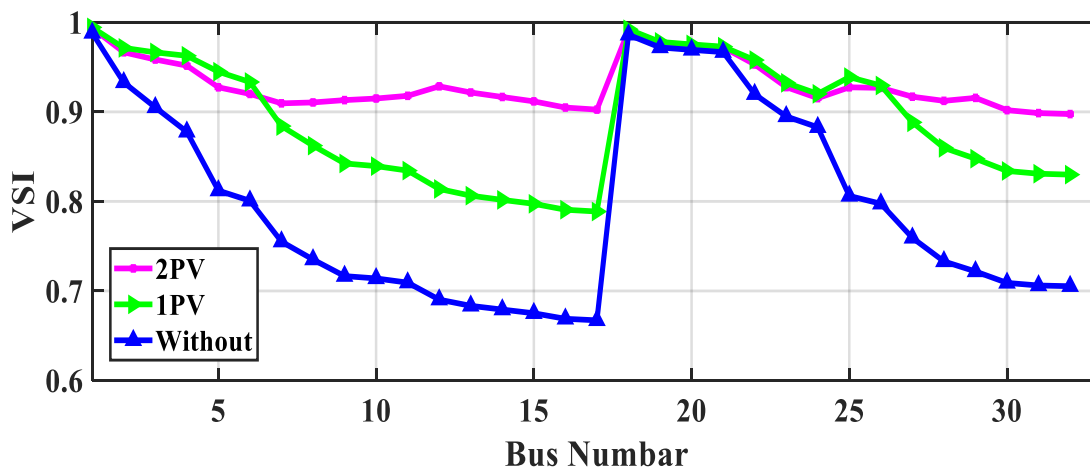


Fig .7. Voltage stability index of the 33 bus system.

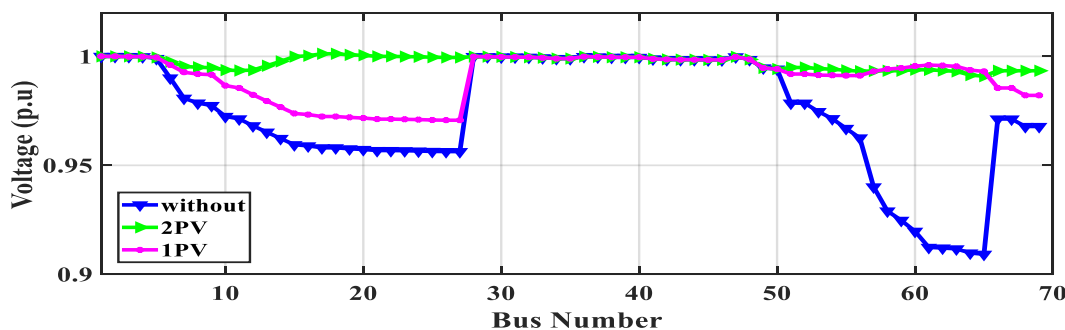


Fig .8. Voltage profile of the 69 bus system.

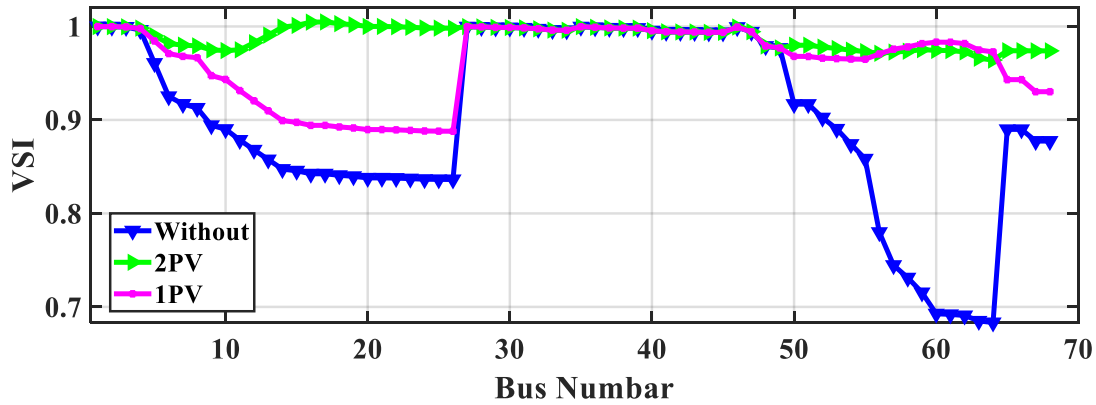


Fig .9. Voltage Stability index of the 69 bus system.

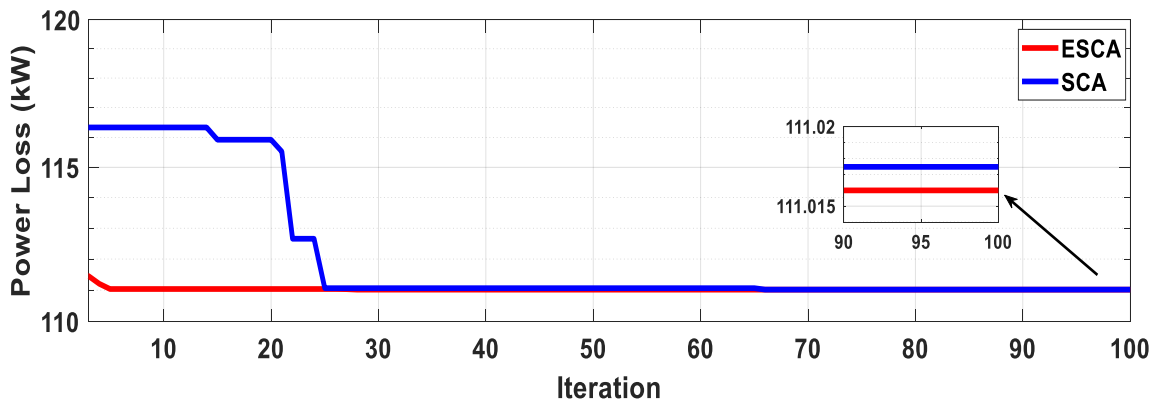


Fig .10. Change of total power loss single PV with iterations for the 33-bus system .

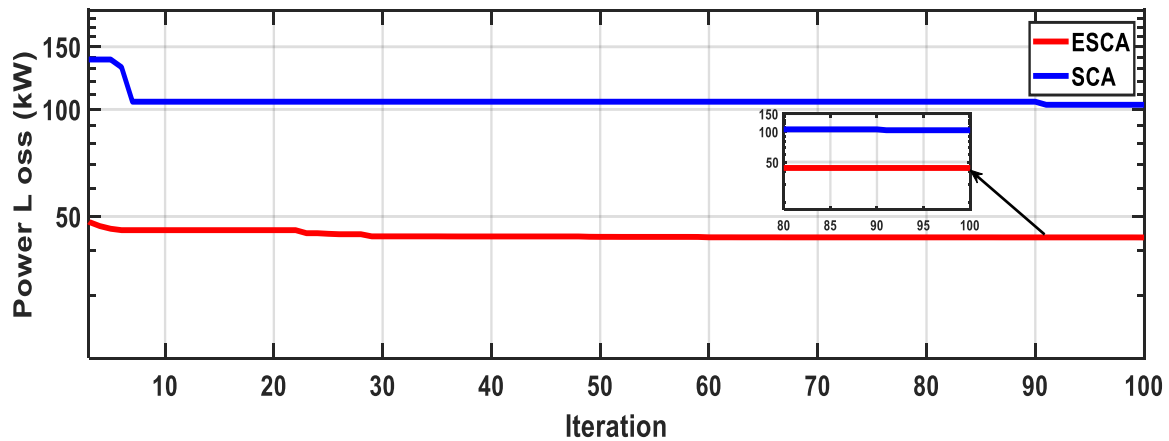


Fig .11. Change of total power loss two PV with iterations for the 33-bus system .

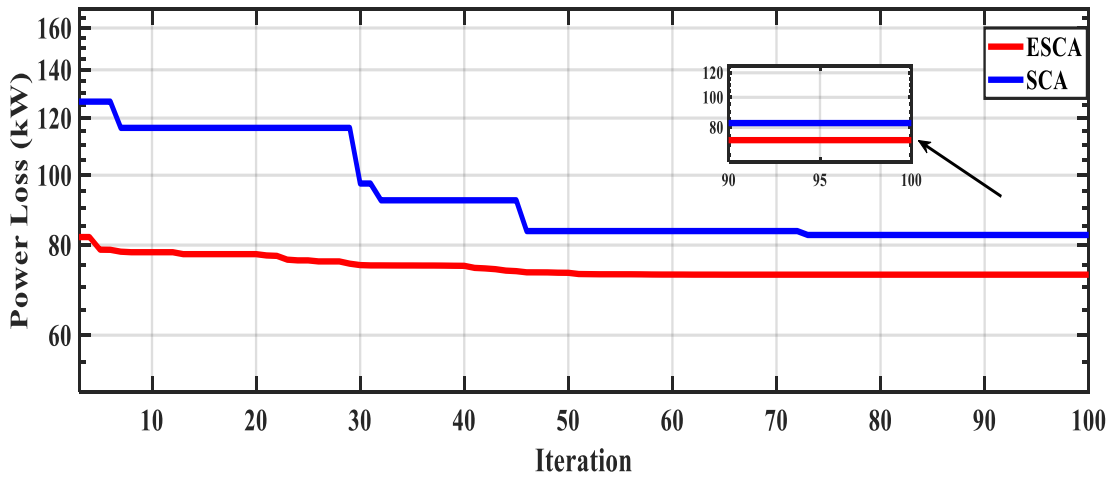


Fig .12. Change of total power loss three PV with iterations for the 33-bus system.

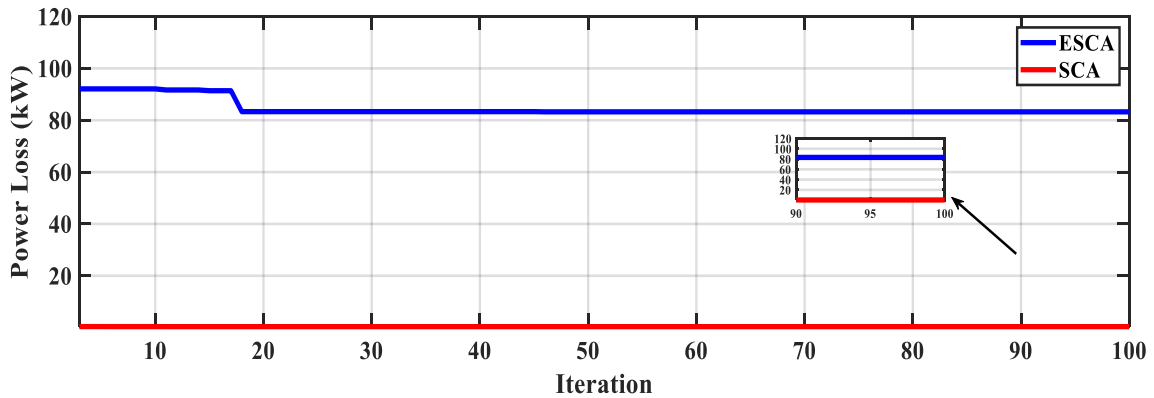


Fig .13. Change of total of total power loss single PV with iterations for the 69-bus system.

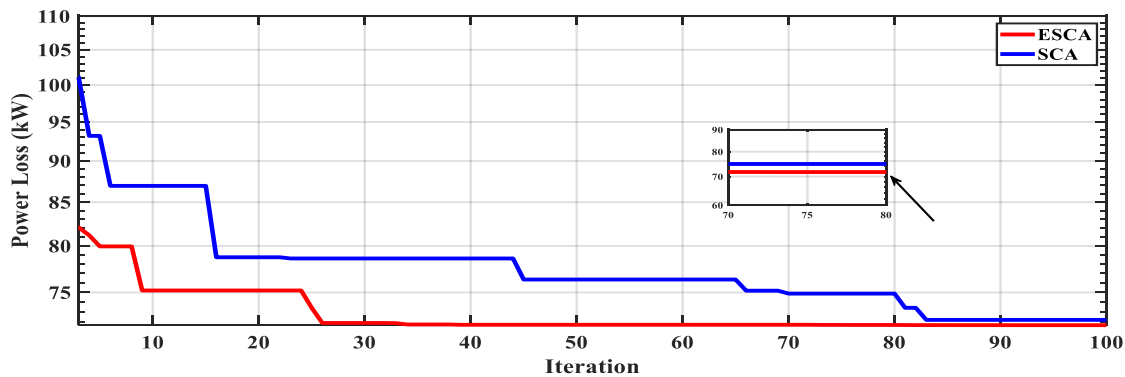


Fig .14. Change of total power loss two PV with iterations for the 69-bus system.

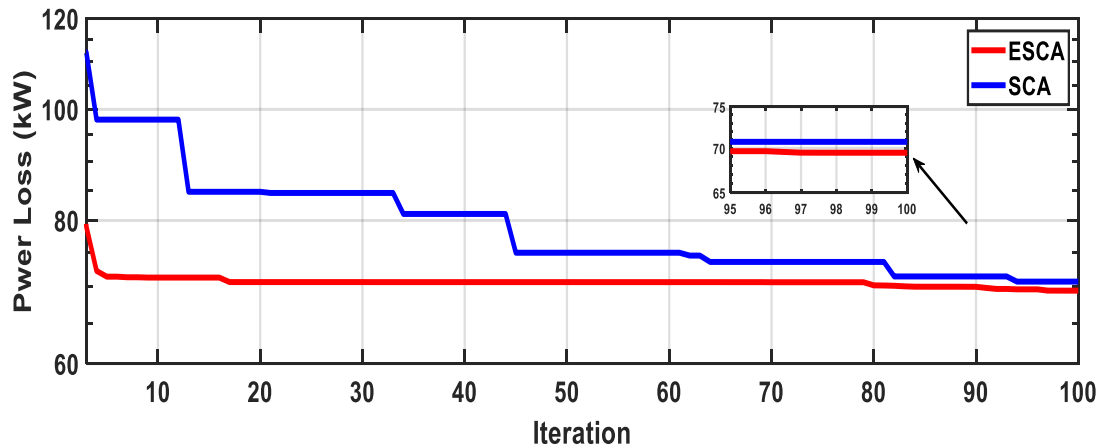


Fig .15. Change of total power loss three PV with iterations for the 69-bus system.

9. Optimal Integral of PV-DGs Along with DSTATCOMs

In this case, PV-DGs and DSTATCOMs are inserted into the IEEE 33 and 69 bus system. The results gained for these cases are listed in Table 13. The optimal position and classifications of the PV-DGs and DSTATCOMs are also qualified. Referring to Table 13, it can be evident that the active power loss has been significantly reduced with 33 bus systems include one PV with one DSTATCOMs to 47.059 kW, and two PVs with two DSTATCOMs to 20.881 kW, respectively. Judging from Table 13, it is evident that the voltage profile and system

stability were greatly improved with simultaneous inclusion of DSTATCOMs and PV-DGs compared to PV inclusion only. Figure 16 and 18 shows the voltage profile of the system with the input of DSTATCOMs and PV-DGs. Figure 17 and 19 illustrates the VSI voltage deviations of the system with the introduction of PV DSTATCOMs. Referring to Table 14, it can be evident that the active power loss has decreased significantly with 69 bus systems comprising one PV with one DSTATCOMs to 14.360kW, and two PVs with two DSTATCOMs to 9.265kW, respectively.

Table 13. Simulation result with inclusion PV and DSTATCOM.

Items	Without – PV 33	With Multi-Objective Function			
		ESCA	SCA	ESCA	SCA
		Single PV & Single DSTATCOM	Two PV & Two DSTATCOM	Single PV & Single DSTATCOM	Two PV & Two DSTATCOM
Total losses (kW)	210.98	58.443	28.882	64.024	30.265

Total Reactive Loss (KVAR)		47.059	20.881	49.646	21.736
Minimum voltage	0.90378 @ bus 18	0.95365 @ bus 18	0.98075 @ bus 25	0.94658 @ bus 18	0.97995 @ bus 18
Maximum voltage	0.99703 @ bus 2	0.99896 @ bus 2	1.00382 @ bus 30	0.99869 @ bus 2	0.99918 @ bus 30
PV size in kW (Location)	-	2531.7 (6)	873.7099 (13), 1192 (30)	2188.7 (6)	743 (12), 1167 (30)
DSTATCOM size in KVA (Location)	-	1256 (30)	460 (23), 1077 (14)	1015 (29)	460 (5), 980 (2)
VSI (p.u)	25.5401	29.8044	31.5515	29.1186	30.8336
VD (p.u)	1.8044	0.5738	0.1453	0.7590	0.2969

Table 14. Simulation result with inclusion PV and DSTATCOM .

Items	Without – PV 69	With Multi-Objective Function			
		ESCA		SCA	
		Single PV & Single DSTATCOM	Two PV & Two DSTATCOM	Single PV & Single DSTATCOM	Two PV & Two DSTATCOM
Total losses (kW)	225	23.441	11.773	26.734	12.477
Total Reactive Loss (KVAR)		14.360	9.265	16.434	10.084
Minimum voltage	0.90919 @ bus 65	0.97306 @ bus 27	0.99427 @ bus 50	0.97054 @ bus 27	0.99313 @ bus 69
Maximum voltage	0.99997 @ bus 2	1.00260 @ bus 62	1.00325 @ bus 14	0.99998 @ bus 2	0.99999 @ bus 2
PV size in kW (Location)	-	1902.2 (61)	1757.5 (61), 835 (13)	1.6430 (61)	380 (21), 1636 (61)
DSTATCOM size in KVA (Location)	-	1353 (61)	1052.8 (10), 757 (56)	1037 (61)	538 (36), 1430 (3)
VSI (p.u)	61.2181	65.8998	67.8398	26.7343	67.3390
VD (p.u)	1.8374	0.5617	0.0755	0.7332	0.1661

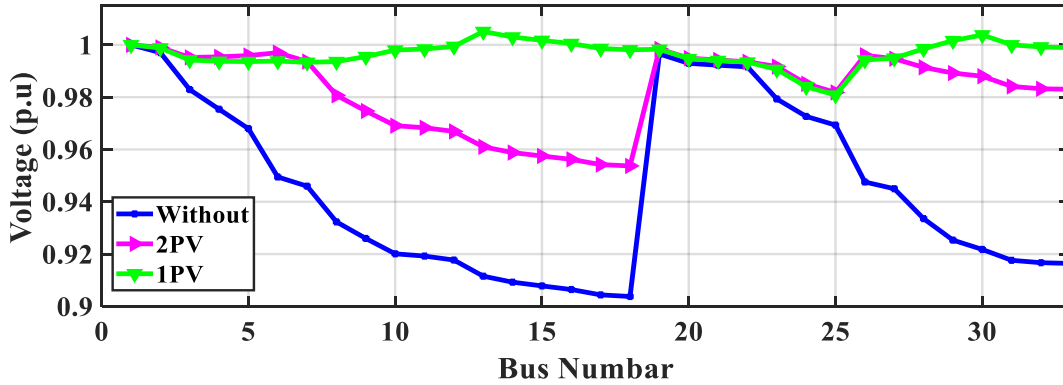


Fig .16. Voltage profile with 33 bus system.

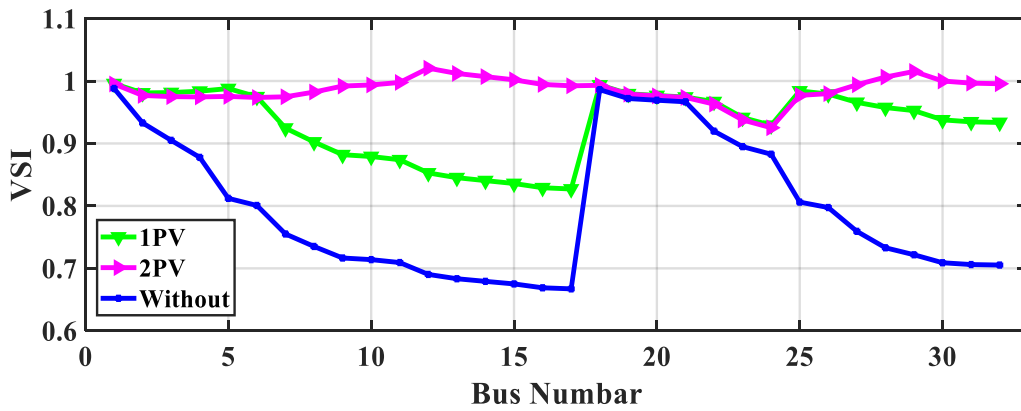


Fig .17. Voltage Stability index with 33 bus system.

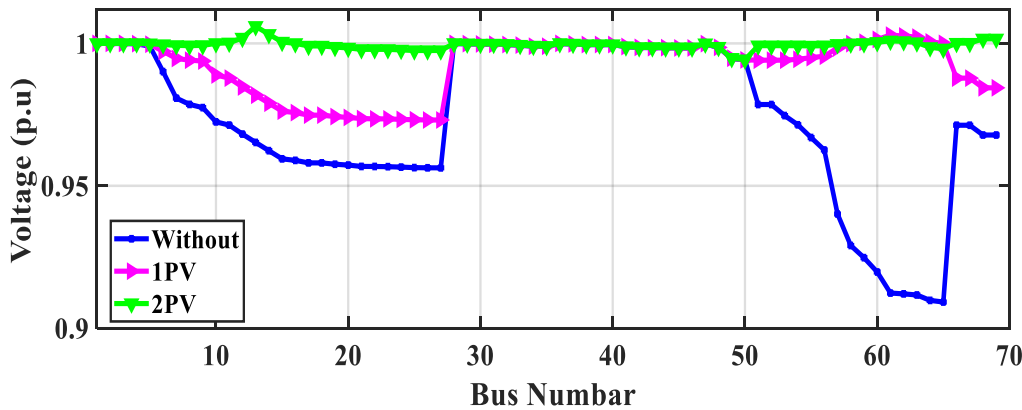


Fig .18. Voltage profile 69 bus system.

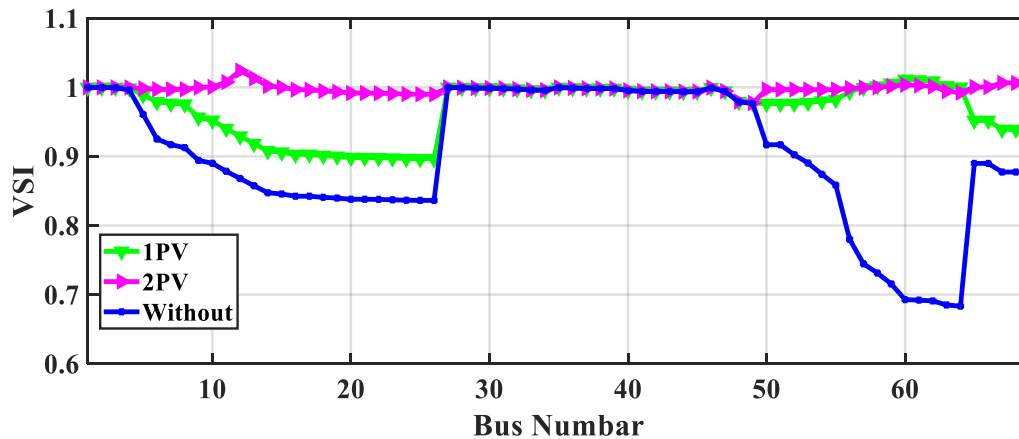


Fig .19. Voltage Stability index with 69 bus system.

Conclusion

This paper proposes a new methodology to determine the optimal sites and sizes of the PV-DG and DSTATCOM in radial distribution system using Enhanced Sine Cosine Algorithm (ESCA). The proposed algorithm is based on the Levy Flight Distribution (LFD) and adaptive operator. to demonstrates effectiveness of the proposed algorithm. The proposed algorithm was tested on the IEEE 33-bus and IEEE 69-bus radial distribution systems and the obtained results have been compared with other algorithms to demonstrate the efficiency and effectiveness of the proposed algorithm. The considered objective function is multi-objective function includes minimizing power losses, minimizing voltage deviations and improving voltage stability. Several studied cases are presented including optimal inclusion of the PV units for power losses only and a comprehensive comparison has been presented using other optimization techniques. In addition of that the PV-DGs and DSTATCOMs have been incorporated with considering the multi-objective function under

single, two and three units of the PV-DGs and DSTATCOMs. The obtained results verified that the proposed algorithm is superior effective for assigning the optimal locations and ratings of the PV-DGs and DSTATCOMs other optimization algorithms. In addition of that inclusion of the PV-DGs and DSTATCOMs can enhance the system performance considerably especially with inclusion of Three PV-DGs and three DSTATCOM compared with other cases.

Reference

- [1] H. Ng, M. Salama, and A. Chikhani, "Classification of capacitor allocation techniques," *IEEE Transactions on power delivery*, vol. 15, pp. 387-392, 2000.
- [2] M. Ebeed, S. Kamel, S. H. A. Aleem, and A. Y. Abdelaziz, "Optimal allocation of compensators," in *Electric Distribution Network Planning*, ed: Springer, 2018, pp. 321-353.
- [3] M. Elkadeem, S. Wang, E. G. Atia, M. Shafik, S. W. Sharshir, Z. Ullah, and H. Chen, "Techno-economic design and

- assessment of grid-isolated hybrid renewable energy system for agriculture sector," in *2019 14th IEEE Conference on Industrial Electronics and Applications (ICIEA)*, 2019, pp. 1562-1568.
- [4] S. Kosai, "Dynamic vulnerability in standalone hybrid renewable energy system," *Energy Conversion and Management*, vol. 180, pp. 258-268, 2019.
- [5] K. Genwa and C. Sagar, "Energy efficiency, solar energy conversion and storage in photogalvanic cell," *Energy conversion and Management*, vol. 66, pp. 121-126, 2013.
- [6] S. Esmaeili, A. Anvari-Moghaddam, and S. Jadid, "Optimal operational scheduling of reconfigurable multi-microgrids considering energy storage systems," *Energies*, vol. 12, p. 1766, 2019.
- [7] J. Najafi, A. Peiravi, A. Anvari-Moghaddam, and J. M. Guerrero, "Resilience improvement planning of power-water distribution systems with multiple microgrids against hurricanes using clean strategies," *Journal of cleaner production*, vol. 223, pp. 109-126, 2019.
- [8] R. O. Bawazir and N. S. Cetin, "Comprehensive overview of optimizing PV-DG allocation in power system and solar energy resource potential assessments," *Energy Reports*, vol. 6, pp. 173-208, 2020.
- [9] G. Pepermans, J. Driesen, D. Haeseldonckx, R. Belmans, and W. D'haeseleer, "Distributed generation: definition, benefits and issues," *Energy policy*, vol. 33, pp. 787-798, 2005.
- [10] I. Pisica, C. Bulac, and M. Eremia, "Optimal distributed generation location and sizing using genetic algorithms," in *2009 15th International Conference on Intelligent System Applications to Power Systems*, 2009, pp. 1-6.
- [11] M. A. Masoum, S. M. M. Badejani, and M. Kalantar, "Optimal placement of hybrid PV-wind systems using genetic algorithm," in *2010 Innovative Smart Grid Technologies (ISGT)*, 2010, pp. 1-5.
- [12] F. S. Abu-Mouti and M. El-Hawary, "Optimal distributed generation allocation and sizing in distribution systems via artificial bee colony algorithm," *IEEE transactions on power delivery*, vol. 26, pp. 2090-2101, 2011.
- [13] A. Ramadan, M. Ebeed, S. Kamel, and L. Nasrat, "Optimal Allocation of Hybrid Solar-Wind Distributed Generations in Distribution Networks Considering the Uncertainty Using Grasshopper optimization Algorithm," in *2019 21st International Middle East Power Systems Conference (MEPCON)*, 2019, pp. 406-410.
- [14] S. Kamel, A. Ramadan, M. Ebeed, L. Nasrat, and M. H. Ahmed, "Sizing and Evaluation Analysis of Hybrid Solar-Wind Distributed Generations in Real Distribution Network Considering the Uncertainty," in *2019 International Conference on Computer, Control,*

- Electrical, and Electronics Engineering (ICCCEEE)*, 2019, pp. 1-5.
- [15] A. Ramadan, M. Ebeed, S. Kamel, and L. Nasrat, "Optimal allocation of renewable energy resources considering uncertainty in load demand and generation," in *2019 IEEE Conference on Power Electronics and Renewable Energy (CPERE)*, 2019, pp. 124-128.
- [16] A. El-Fergany, "Optimal allocation of multi-type distributed generators using backtracking search optimization algorithm," *International Journal of Electrical Power & Energy Systems*, vol. 64, pp. 1197-1205, 2015.
- [17] E. Ali, S. A. Elazim, and A. Abdelaziz, "Ant lion optimization algorithm for renewable distributed generations," *Energy*, vol. 116, pp. 445-458, 2016.
- [18] S. Mirjalili, "SCA: a sine cosine algorithm for solving optimization problems," *Knowledge-based systems*, vol. 96, pp. 120-133, 2016.
- [19] X.-S. Yang and S. Deb, "Cuckoo search via Lévy flights," in *2009 World congress on nature & biologically inspired computing (NaBIC)*, 2009, pp. 210-214.
- [20] A. El-Fergany, "Study impact of various load models on DG placement and sizing using backtracking search algorithm," *Applied Soft Computing*, vol. 30, pp. 803-811, 2015.
- [21] D. Thukaram, H. W. Banda, and J. Jerome, "A robust three phase power flow algorithm for radial distribution systems," *Electric Power Systems Research*, vol. 50, pp. 227-236, 1999.
- [22] G. Chang, S. Chu, and H. Wang, "An improved backward/forward sweep load flow algorithm for radial distribution systems," *IEEE Transactions on power systems*, vol. 22, pp. 882-884, 2007.
- [23] A. A. Hassan, F. H. Fahmy, A. E.-S. A. Nafeh, and M. A. Abu-elmagd, "Genetic single objective optimisation for sizing and allocation of renewable DG systems," *International Journal of Sustainable Energy*, vol. 36, pp. 545-562, 2017.
- [24] H. Manafi, N. Ghadimi, M. Ojaroudi, and P. Farhadi, "Optimal placement of distributed generations in radial distribution systems using various PSO and DE algorithms," *Elektronika ir Elektrotechnika*, vol. 19, pp. 53-57, 2013.
- [25] N. Acharya, P. Mahat, and N. Mithulananthan, "An analytical approach for DG allocation in primary distribution network," *International Journal of Electrical Power & Energy Systems*, vol. 28, pp. 669-678, 2006.
- [26] T. Shukla, S. Singh, V. Srinivasarao, and K. Naik, "Optimal sizing of distributed generation placed on radial distribution systems," *Electric power components and systems*, vol. 38, pp. 260-274, 2010.
- [27] S. G. Naik, D. Khatod, and M. Sharma, "Optimal allocation of combined DG and capacitor for real power loss minimization in distribution networks," *International Journal of Electrical Power & Energy Systems*, vol. 53, pp. 967-973, 2013.

- [28] S. Kaur, G. Kumbhar, and J. Sharma, "A MINLP technique for optimal placement of multiple DG units in distribution systems," *International Journal of Electrical Power & Energy Systems*, vol. 63, pp. 609-617, 2014.
- [29] K. Mahmoud, N. Yorino, and A. Ahmed, "Optimal distributed generation allocation in distribution systems for loss minimization," *IEEE Transactions on Power Systems*, vol. 31, pp. 960-969, 2015.
- [30] S. Kansal, V. Kumar, and B. Tyagi, "Hybrid approach for optimal placement of multiple DGs of multiple types in distribution networks," *International Journal of Electrical Power & Energy Systems*, vol. 75, pp. 226-235, 2016.
- [31] D. Q. Hung and N. Mithulananthan, "Multiple distributed generator placement in primary distribution networks for loss reduction," *IEEE Transactions on industrial electronics*, vol. 60, pp. 1700-1708, 2011.
- [32] J. A. M. García and A. J. G. Mena, "Optimal distributed generation location and size using a modified teaching-learning based optimization algorithm," *International journal of electrical power & energy systems*, vol. 50, pp. 65-75, 2013.
- [33] M. Kefayat, A. L. Ara, and S. N. Niaki, "A hybrid of ant colony optimization and artificial bee colony algorithm for probabilistic optimal placement and sizing of distributed energy resources," *Energy Conversion and Management*, vol. 92, pp. 149-161, 2015.
- [34] W. Tan, M. Hassan, M. Majid, and H. Rahman, "Allocation and sizing of DG using cuckoo search algorithm," in *2012 IEEE international conference on power and energy (PECon)*, 2012, pp. 133-138.
- [35] S. Kamel, A. Amin, A. Selim, and M. H. Ahmed, "Optimal Placement of DG and Capacitor in Radial Distribution Systems Considering Load Variation," in *2019 International Conference on Computer, Control, Electrical, and Electronics Engineering (ICCCEEE)*, 2019, pp. 1-6.